



NASA TECHNICAL NOTE

NASA TN D-3928

NASA TN D-3928

W 67-23301

FACILITY FORM 602

(ACCESSION NUMBER)

(THRU)

31
(PAGES)

15
(COPIES)

(NASA CR OR TMX OR AD NUMBER)

(CATEGORY)

OPERATION OF HYDRODYNAMIC JOURNAL BEARINGS IN SODIUM AT TEMPERATURES TO 800° F AND SPEEDS TO 12 000 RPM

*by Fredrick T. Schuller, William J. Anderson,
and Zolton Nemeth*

*Lewis Research Center
Cleveland, Ohio*

OPERATION OF HYDRODYNAMIC JOURNAL BEARINGS
IN SODIUM AT TEMPERATURES TO 800° F
AND SPEEDS TO 12 000 RPM

By Fredrick T. Schuller, William J. Anderson,
and Zolton Nemeth

Lewis Research Center
Cleveland, Ohio

NATIONAL AERONAUTICS AND SPACE ADMINISTRATION

OPERATION OF HYDRODYNAMIC JOURNAL BEARINGS
IN SODIUM AT TEMPERATURES TO 800⁰ F
AND SPEEDS TO 12 000 RPM

by Fredrick T. Schuller, William J. Anderson,
and Zolton Nemeth

Lewis Research Center

SUMMARY

A series of experiments was conducted with 1.5-inch-diameter hydrodynamic journal bearings in liquid sodium at 500⁰ and 800⁰ F at speeds to 12 000 rpm with unit loads to 31.1 pounds per square inch. Bearings of five different configurations were tested. Tilting-pad bearings were the most stable, followed in order by (1) a plain cylindrical bearing with a herringbone-groove journal, (2) a three-axial-groove cylindrical bearing, pressure fed from an axial shaft pump through a hole in the journal, and (3) three- and two-axial-groove cylindrical bearings.

Stellite Star J material mated with Hastelloy X, titanium carbide (K184B), or Inconel had the best wear and seizure properties. Also titanium carbide (K184B) mated with a molybdenum-0.5 percent titanium alloy showed excellent promise. Surface damage to the tilting-pad-bearing pivots was observed in some tests, even after short runs at light loads. Existing theory is adequate for predicting the onset of instability in circular, axially grooved bearings.

INTRODUCTION

Extended space exploration missions of the future will necessitate long periods of continuous, reliable operation of the power generation system in the space vehicle. Power levels of 30 000 watts to the million watt range are anticipated (ref. 1). At the present time, it appears that a turbogenerator system that employs a liquid metal as the working fluid is the most advantageous system for the high power levels desired. Requirements for light weight, high reliability, and minimum complexity dictate the use of

a hermetically sealed pump, with process-fluid lubricated bearings, to circulate the fluid through the entire system, including the space radiator.

Fluid-film bearings have been selected over rolling-element bearings because the former bearing type maintains a full fluid film more easily. This film eliminates or minimizes the rubbing-contact problem that is usually present in rolling-element bearings. Also, the materials problem in fluid-film bearings is much simpler because of less stringent hardness requirements.

Fluid-film bearings do, however, have the following disadvantages: increased power losses, greater breakaway torques, and the need for a separate bearing to carry thrust loads. The disadvantage of principal interest here is the tendency of fluid-film bearings to exhibit instability under the light- or zero-load conditions that will exist in a space vehicle in a zero-gravity environment. Instability here refers to half-frequency whirl, or the tendency of the journal center to orbit the bearing center at an angular velocity about half that of the journal around its own center.

Materials chosen as bearing and journal pairs in an alkali-metal system must have resistance to corrosion in the liquid, good wear and seizure resistance, and a low coefficient of friction to ensure reasonable breakaway torque. A survey of existing literature on the usefulness of materials for bearings in liquid alkali metals (refs. 2 to 4) and the need for using materials of particular expansion coefficients led to the selection of the bearing and journal materials reported herein.

This investigation was conducted to determine the stability characteristics of five bearing configurations and the compatibility and wear and seizure resistance of various bearing and journal material combinations in liquid sodium at temperatures to 800° F. The bearings with 1.5-inch bore by 1.5-inch length were submerged in liquid sodium and operated hydrodynamically at radial loads from zero to 31.1 pounds per square inch and journal speeds to 12 000 rpm at 500° and 800° F. Bearing friction torque at varying speeds and loads was recorded and compared with theoretical values under both laminar and turbulent flow conditions.

TEST BEARINGS

Design

Hydrodynamic bearings of five configurations were tested fully immersed in liquid sodium (fig. 1). Bearings with two or three axial grooves, a herringbone-groove journal with a plain bearing, and a three-tilting-pad bearing were evaluated. A three-groove bearing with a circumferential feed groove was run with an axial flow pump attached to the test shaft, which pressure fed the test bearing through a hole in the test journal.

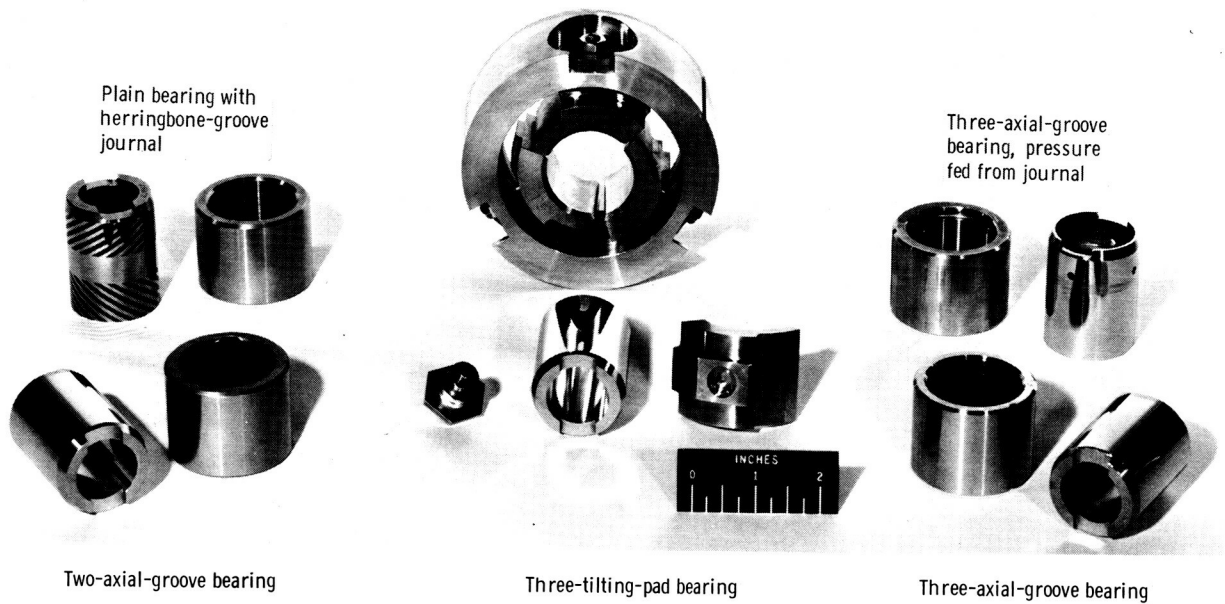


Figure 1. - Bearing configurations.

CS-66-2734

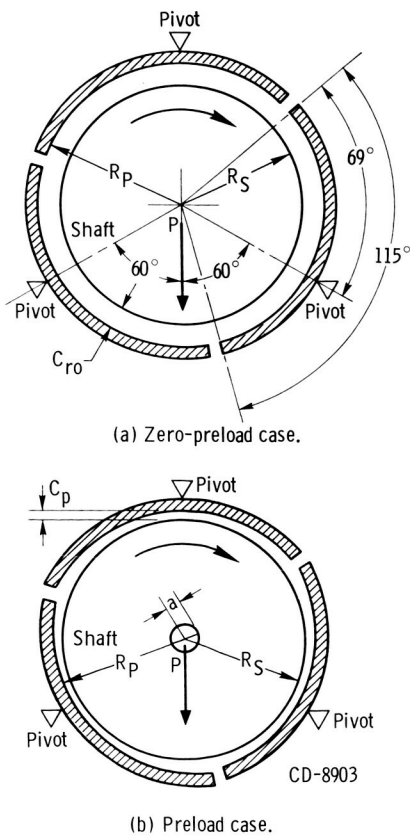


Figure 2. - Tilting-pad-bearing geometry before and after preload. Bearing radial clearance at zero preload, $C_{ro} = R_p - R_s$; bearing radial clearance at pivot location after preload, $C_p = R_p - a - R_s$; preload, a ; preload coefficient, $a/R_p - R_s$.

The bore and length of the bearings in all cases were nominally 1.5 inches. The journal outside diameter and bearing inside diameter were machined to a 4 to 8 microinch rms finish.

A schematic diagram of a tilting-pad bearing with and without geometric preload is presented in figure 2. Preload is used to achieve high bearing stiffness, even with zero net load on the shaft, and to ensure that positive fluid-film pressures act on all the bearing pads. If a pad is allowed to become completely unloaded, it may flutter and contact the journal. Preload 'a' is the radial distance that the pad pivots are mechanically displaced toward the center of the journal from their original concentric position. The preload coefficient $a/(R_p - R_s)$ is the fraction of the radial clearance that the pads are displaced toward the center of the journal from their original concentric position. A preload coefficient of 1.00 would therefore mean that the pads would be touching the journal at their pivot locations.

A three-pad configuration was chosen because it affords greater load capacity than a configuration of

more than three pads. Also, it is much easier to align all pivot points accurately on the common pivot circle center with a three-pad configuration than with one of more than three pads.

Load is applied symmetrically between two support points (pivots) (fig. 2) because maximum load capacity is obtained with this arrangement when a unidirectional load is employed. For maximum load-carrying capacity, with an incompressible fluid, the pivots should be located 0.6 of the full arc length from the leading edge of the pads ($69^\circ/115^\circ = 0.6$, fig. 2).

Materials

The bearing and journal materials were Stellite Star J, molybdenum-0.5 percent titanium, Hastelloy X, Inconel, and titanium carbide (K184B). The composition and hardness of these materials are given in table I.

TABLE I. - NOMINAL COMPOSITION AND HARDNESS OF BEARING AND JOURNAL MATERIALS

Materials	Rockwell hardness at room temperature	Alu- mi- num	Car- bon	Chro- mium	Co- balt	Iron	Man- ga- nese	Nickel	Sili- con	Tung- sten	Tita- nium	Tita- nium car- bide	Molyb- denum	Others
		Concentration, percent												
Stellite Star J	C-62	---	2.5	32	40.5	3	---	2.5	---	17	---	--	---	2.5
Hastelloy X	B-87	---	.2	22	1.5	18	---	47.2	---	.6	---	--	9	1.5
Molybdenum - 0.5 percent titanium	B-87	---	---	--	---	--	---	---	---	---	0.5	--	99.5	---
Inconel	B-75 to B-95	---	.04	15	---	7	0.35	78	0.20	---	---	--	---	---
Titanium carbide (K184B; nickel bonded)	C-67	3	---	3	---	--	---	40	---	---	---	50	4	---

APPARATUS

Bearing Test Apparatus

A section of the test vessel and the radial loading system is shown schematically in figure 3(a). The test bearing was mounted in a housing in the test vessel, and the test journal was mounted and keyed to the bottom end of the test shaft. A cutaway view of the bearing test apparatus, shown in figure 3(b), illustrates the configuration in detail. The test shaft was positioned vertically so that normal gravity forces would not act on the journal. A 15-horsepower direct-current motor powered the test shaft through a 7.5 to 1 ratio gearbox. The sodium test vessel was located immediately below the main support-bearing housing and floated between the upper and lower gas bearings. Two semicircular wheels connected by a cable belt comprised the radial loading system. Radial load was applied by an air cylinder between the two semicircular wheels, one of which pivots on a knife edge. Bearing torque was measured by a force transducer. Vertical positioning of the test vessel was achieved by a vertically mounted air cylinder located below the vessel.

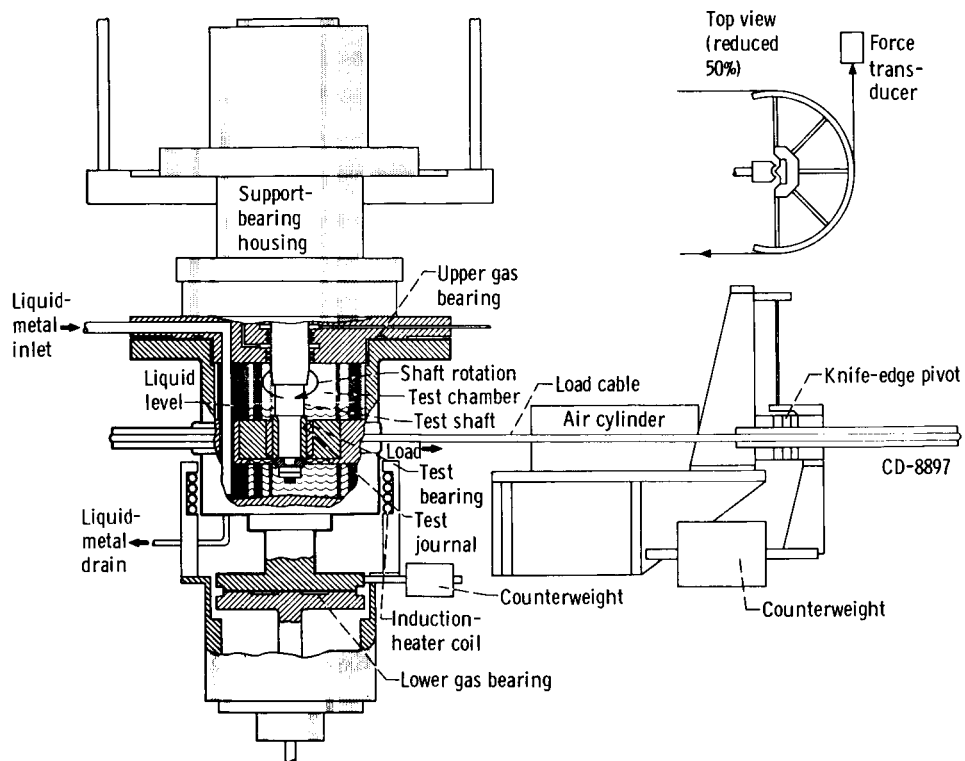
The test shaft was mounted on two support ball bearings (fig. 3(b)) that were preloaded to about 40 pounds by a wave spring. This preload was necessary to ensure a minimum amount of test-shaft runout. Cooling fins were mounted on the test shaft immediately below the bottom support bearing to dissipate heat and prevent excessive lower-support-bearing temperatures due to soak back from the high temperature sodium in the test vessel.

Liquid sodium at 400° F was introduced to the test vessel and heated to the desired test temperature by an induction heater. The induction-heater coil around the test vessel (fig. 3(a)) did not come into physical contact with the outer surface of the test vessel; therefore, the free-swinging motion of the test vessel was not inhibited. A drain was provided at the bottom of the test vessel to facilitate elimination of the contaminated sodium.

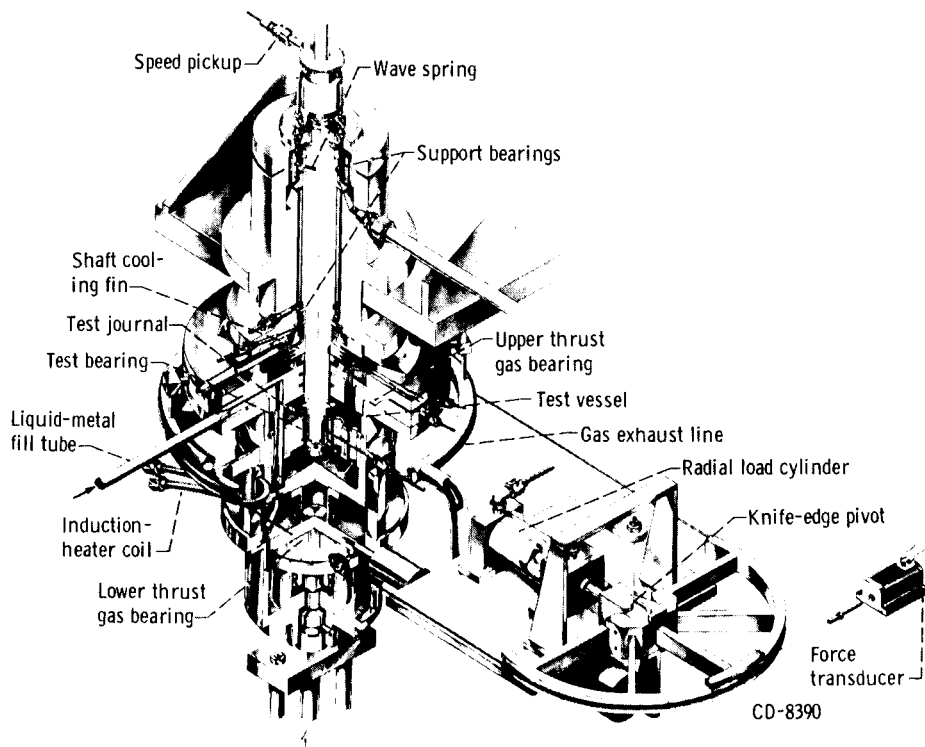
Sodium Supply System

The sodium supply system, shown schematically in figure 4, was designed as a non-circulating system composed of a supply tank, supply line, sodium filter, filter bypass line, control valve, and sample trap.

The supply tank was designed to contain 20 gallons of sodium and was equipped with a fill valve, dual thermowells, a diffusional cold trap, a pressure transmitter, a vapor trap, and a sodium supply line. The liquid metal was supplied to the bearing test



(a) Detailed view of bearing test installation.



(b) Cutaway view.

Figure 3. - Liquid-metal bearing apparatus.

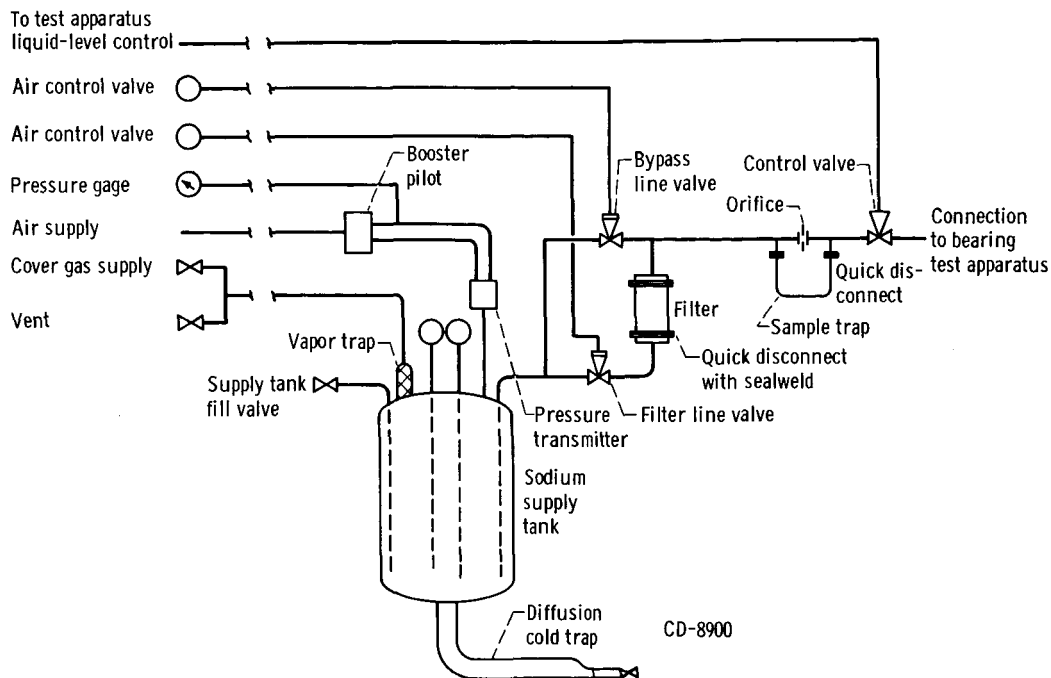


Figure 4. - Liquid-metal supply system for bearing test apparatus.

apparatus by a differential pressure between the tank and the bearing test apparatus. A diffusional cold trap was provided to control the sodium oxide content during operation of the sodium system. The cold trap was an uninsulated appendage connected to the bottom of the supply tank, which was designed so that the end of this unit would be at the lowest temperature in the entire system. Sodium oxide is the major detrimental contaminant of a sodium liquid-metal system, and its solubility in sodium is temperature dependent; therefore, it diffuses to the location having the lowest temperature. The cover gas for pressurizing and venting the supply tank was passed through a wire-mesh demister (vapor trap) that prevented any sodium vapors from getting into the cover-gas system.

A micrometallic filter was provided in the supply line to the bearing test apparatus to permit continuous filtering of all supply sodium. The porous micrometallic filter unit was designed so that the filtering element could be replaced.

Five valves were incorporated in the sodium supply system:

- (1) A control valve to control flow to the bearing test apparatus by liquid-level probes in the test vessel
- (2) A bypass-line valve to direct the flow either through or around the filter, as desired
- (3) A filter-line valve to direct the flow through the filter (the bypass valve must be closed in this case)
- (4) A fill valve to control filling the 20-gallon supply tank
- (5) A cold-trap drain valve to control draining the cold trap

Instrumentation

A dual Chromel-Alumel thermocouple was attached to the back of the test bearing. Another dual Chromel-Alumel thermocouple extended into the liquid sodium in the test vessel and controlled the induction heater.

Two capacitance probes, which measured the movement of the test vessel during a test, were mounted outside the test vessel on the vessel cover, at 90° from each other. The signal from the probes was fed through displacement meters to an x-y display in an oscilloscope where the actual pattern of motion of the test vessel could be observed. The orbital frequency of the test vessel was measured by a frequency counter. Actual bearing clearance was obtained at test temperature by measurement of the figure generated on the oscilloscope screen as the test vessel was moved, by hand, to the limits of its outward motion in a circular orbit about the stationary journal.

Test shaft speed was measured with a magnetic pickup head mounted close to a six-toothed gear on the test shaft. The signal from the pickup was displayed on a four-channel frequency counter.

PROCEDURE

Pretest Preparation for Two- and Three-Axial-Groove Bearings

Prior to each test, the test bearing was assembled into its housing with a slight interference fit. The bearing was then machined in place to a predetermined inside diameter at room temperature that would result in the desired bore size at test temperature. Nine bore-gage readings, each accurate to within 0.0001 inch, were averaged and used as a measure of the bearing bore. The outside diameter of the mating journal was then ground to a size that would result in the desired clearance for the test bearing. The journal outside diameter was machined to within 0.0002 inch concentricity with its inside diameter to ensure a minimum amount of runout.

The test-bearing housing was then assembled in the test vessel which was carefully raised into position around the test journal on the shaft by the lower air cylinder.

Pretest Preparation for Tilting-Pad Bearings

The radii of the three pads of the tilting-pad-bearing assembly were checked after delivery from the manufacturer to ensure an accurate geometry. The pads were assembled into an annular housing by a threaded pivot and nut arrangement (fig. 5).

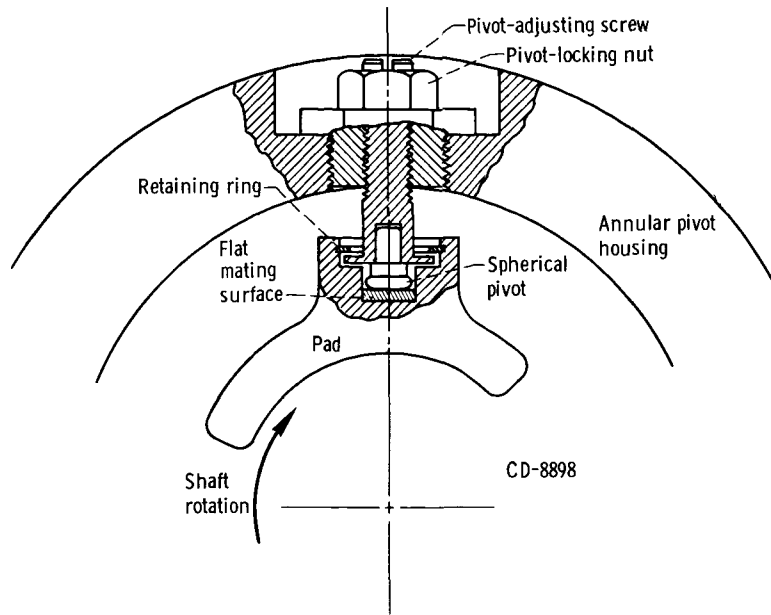


Figure 5. - Section view of tilting-pad bearing assembly.

Desired preload was obtained by adjustment of the threaded pivots until the bearing surfaces of the pads made intimate contact around a presized setup plug. The plug was then removed, and the tilting-pad housing was assembled into the test vessel which was carefully raised into test position around the journal.

General Pretest Preparation

After the bearing and journal were assembled and the test vessel was raised to its test position with the upper and lower gas bearings turned on, the test vessel was filled with alcohol and drained as a final cold cleaning procedure. The test vessel was then purged with argon. A cover gas of argon was supplied to the test vessel throughout the experiment. The test vessel was preheated to 500^o F. Then liquid sodium at about 400^o F and under a pressure of about 5 pounds per square inch was introduced into the test vessel from the 20-gallon supply system. Sodium flowed into the test vessel until it made contact with the liquid-level probe, which automatically closed the main sodium supply valve to prevent overfilling.

With the bearing and journal completely submerged in sodium, the test vessel was heated to 500^o F and allowed to soak for approximately 4 hours to remove the remaining contaminants. The vessel was then drained and refilled with clean sodium. The bearing test was started after equilibrium conditions had been attained at the desired test temperature.

TABLE II. - RESULTS OF TESTS OF TWO- AND THREE-GROOVE BEARINGS IN SODIUM

Bearing Number	Bearing Material	Journal		Bearing type	Test temperature, °F	Measured ^a radial clearance at test temperature, in.	Journal speed range tested, rpm	Unit load range tested, psi	Total test time, min	Observed instability	Remarks
		Number	Material								
M-1	Molybdenum - 0.5 percent titanium	K-6	Titanium carbide	Two groove	500	0.0010	3 000 to 8 000	4.5 to 20.0	470	At various speed and load conditions	Bearing and journal showed moderate wear due to half-frequency whirl. Increasing load stabilized bearing. Bearing did not seize; deliberate half-frequency-whirl operation run at momentary intervals.
M-7	Molybdenum - 0.5 percent titanium	K-B	Titanium carbide	Two groove	800	0.0010	4 000 to 11 000	4.5 to 20.0	703	None present	Bearing showed moderate wear at both ends indicating that the test vessel had cocked; bearing did not seize. Sodium had migrated to top gas bearing of test vessel.
J-1	Stellite Star J	HX-B	Hastelloy X	Three groove	500	0.0013	5 000	22.0	5	Not set up to observe	Contaminant particle scored bearing and caused seizure almost immediately after start of test.
J-2	Stellite Star J	HX-C	Hastelloy X	Three groove	500	0.0012	5 000 to 7 000	11.0	257	At 7000 rpm and 11.0 psi load	Bearing and journal showed severe wear but no seizure resulted. Bearing deliberately held at 7000 rpm and 11.0 psi for 90 minutes to observe results of half-frequency-whirl operation.
J-3	Stellite Star J	HX-D	Hastelloy X	Three groove	500	0.0011	5 000 to 7 000	9.0	260	Not set up to observe	Bearing and journal showed heavy wear probably due to unstable operation at light load. Bearing did not seize.
HX-B	Hastelloy X	J-5	Stellite Star J	Three groove	500	0.0011	5 000	11.0	30	Not set up to observe	Bearing seized after 30 min, apparently because of contaminant particle.
HX-D	Hastelloy X	J-6	Stellite Star J	Three groove	500	0.0015	3 000 to 7 000	4.5 to 8.9	460	Not set up to observe	Bearing and journal showed heavy wear but did not seize. Light loads probably caused the bearing to run unstably.
HX-5	Hastelloy X	J-3	Stellite Star J	Three groove	800	0.0008	5 000	Not recorded	Not recorded	Too short a run to observe	Bearing seized immediately, probably because of contaminant particle. Bearing showed a score mark completely around on one end.

K-3	Titanium	J-7	Stellite Star J	Three groove	500	0.0017	5 000	4.5	315	Not set up to ob- serve	Bearing and journal showed heavy wear but did not seize. Bearing apparently was operating unstably because of light load.
M-9	Molybdenum - 0.5 percent titanium	J-11	Stellite Star J	Three groove	500	0.0010	5 000 to 10 000	11.0 to 26.7	290	At various speed and load condi- tions	Bearing and journal showed discoloration but no measurable wear. Bearing was purposely loaded enough to keep it running stably. Deliberate half-frequency-whirl operation run at momentary intervals.
M-12	Molybdenum - 0.5 percent titanium	J-1	Stellite Star J	Three groove	800	0.0011	5 000 to 10 000	13.3 to 22.2	355	None present	Bearing was loaded enough to keep it running stably; however, bearing seized at 8000 rpm during shutdown. Call mark 1/8 in. around bearing possibly caused by contaminant par- ticle or light wear.
M-10	Molybdenum - 0.5 percent titanium	J-2	Stellite Star J	Three groove	800	0.0010	4 000 to 7 000	15.5 to 17.8	242	None present	Bearing seized at 7000 rpm and 17.8 psi load. Two small wear areas on each end of bearing indicated that the test vessel had cocked.
M-11	Molybdenum - 0.5 percent titanium	HX-7	Hastelloy X	Three groove	800	0.0013	Not re- cord- ed	0	Not re- cord- ed	Present imme- diately	Bearing seized immediately at zero load with definite indication of half-frequency whirl. Wear on both ends of bearing was observed.
HX-7	Hastelloy X	J-8	Stellite Star J	Three groove, with screw pump on shaft	500	0.0012	4 000 to 9 000	13.3 to 22.2	647	At various speed and load condi- tions	A shaft screw pump forced sodium into the bearing through a hole in the journal. Bear- ing showed small wear area in loaded zone, probably because of deliberate half- frequency-whirl operation at momentary intervals.

^aMeasured by observation of oscilloscope pattern as the test vessel was moved by hand, to the limits of its outward motion, in a circular orbit about the stationary journal.

Test Procedure

Two types of tests were conducted, one with load and the other at zero-load conditions. Under zero-load conditions, the semicircular wheel that pivots on a knife edge was removed along with its loading cable. The force transducer for torque measurement was attached directly to the semicircular wheel on the test vessel.

Shaft speed was increased in 1000-rpm increments from 3000 to a maximum of 12 000 rpm. In the loaded-bearing tests, the loads were changed as required to fulfill the purpose of the particular test run. In some tests, the load had to be changed to maintain bearing stability, and in others, the load was left unchanged to observe the effect of prolonged instability in a bearing. The time interval between speed and load changes varied but was of sufficient duration to allow the friction torque to stabilize. Speed, load, bearing temperature, and bearing friction torque were recorded at each speed and load condition. Test vessel movement was noted by observation of the oscilloscope screen in an effort to identify bearing instability at each test interval.

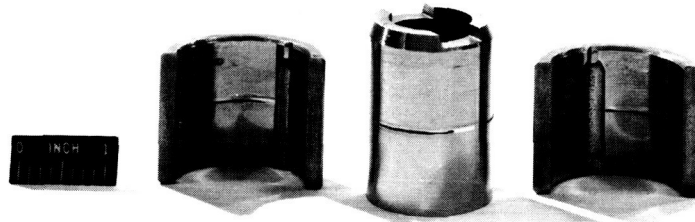
A test was terminated (1) if the bearing seized, (2) if the bearing showed indications of imminent failure by erratic or excessively high torque, (3) if the test vessel no longer floated freely on its gas bearings, or (4) if the desired objective of the test had been attained.

RESULTS AND DISCUSSION

Two- and Three-Axial-Groove Cylindrical Bearings

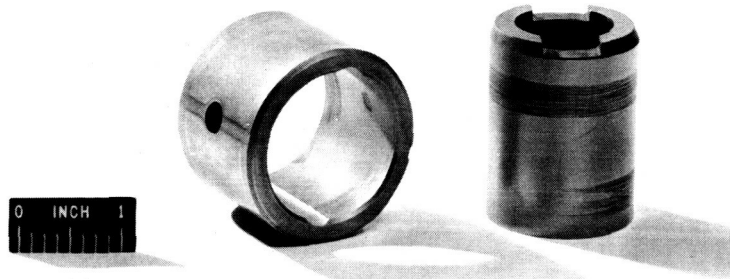
The results of tests on 14 two- and three-axial-groove bearings are summarized in table II. The results of these tests, which were conducted over a speed range from 3000 to 11 000 rpm at unit loads from zero to 26.7 pounds per square inch, were generally poor. Some apparatus problems were encountered in the early phase of the test program. These problems included test-vessel cocking, which caused two failures, and contamination of the sodium, which may have caused four failures due to particle ingestion into the test-bearing clearance area. In three instances, sodium migrated into the upper gas bearing, which caused the test vessel to cock, producing erratic torque readings.

A typical failure caused by contaminant particle ingestion is shown in figure 6. This type of failure resulted in a rather pronounced gouge in the bearings and journal. It was after this type of failure that a cleaning procedure was adopted in which the test bearing and journal in the test vessel were soaked for 4 hours in the sodium bath at 500° F. The contaminated sodium was then drained, and a clean supply of filtered sodium was intro-



C-66-2144

Figure 6. - Seizure caused by contaminant particle. Bearing J-1 against journal HX-B.



C-66-113

Figure 7. - Seizure due to test-vessel cocking. Bearing M-7 against journal K-B.

duced into the test vessel before a test was begun. The orange-peel surface effect shown at the bottom of the bearing grooves in figure 6 was caused by the manufacturing techniques employed in the fabrication of the test bearings.

In some instances, at the higher speeds, excessive sloshing of sodium in the test vessel caused some to migrate into the top gas bearing of the test vessel. These sodium droplets would solidify and test-vessel cocking would result causing the type of failure shown in figure 7 in which wear areas are indicated on both ends of the bearing.

The generally poor results obtained with the two- and three-axial-groove bearings were caused principally by their inherent instability, which is discussed in the section Bearing Instability.

Herringbone-Journal Bearing

Table III summarizes the results of experiments with two herringbone-groove journals running in plain cylindrical bearings. These bearings, one of which is illustrated in figure 8, were tested to determine their stability characteristics. The two herringbone-journal bearings were run over a speed range from 4000 to 12 000 rpm at loads from zero to 20 pounds per square inch at sodium temperatures of 500⁰ and 800⁰ F. Higher bearing torques were observed than for the two- and three-axial-groove bearings because

TABLE III. - RESULTS OF TESTS OF PLAIN CYLINDRICAL BEARINGS AND HERRINGBONE-GROOVE JOURNALS IN SODIUM

Bearing Num- ber	Material	Journal		Bearing type	Test tem- pera- ture, °F	Measured ^a radial clearance at test tempera- ture (on lands), °F	Journal speed- range tested, rpm	Unit load- range tested, psi	Total test time, min	Groove angle meas- ured from a perpen- dicular to the journal axis, β , deg	Number of grooves and lands	Width of grooves and lands, in.	Depth of grooves, in.	Observed instability	Remarks
		Num- ber	Mate- rial												
MP-3	Molybdenum - 0.5 percent titanium	K-14	Tita- nium car- bide	Plain bear- ing with herringbone- groove journal	500	0.0013	4 000 to 12 000	b ₀ to 17.8	490	33	20	0.064	0.0014	At various speed and load condi- tions	Light wear in bear- ing and journal caused by delib- erate half- frequency-whirl operation at momentary in- tervals.
MP-4	Molybdenum - 0.5 percent titanium	K-A	Tita- nium car- bide	Plain bear- ing with herringbone- groove journal	800	0.0008	5 000 to 7 000	b ₀ to 20.0	90	33	20	0.064	0.0014	At 5000 rpm and zero load	Bearing seized be- cause of overload caused by heater expansion which pushed the test vessel and in- creased the radial load.

^aMeasured by observation of oscilloscope pattern as the test vessel was moved by hand, to the limits of its outward motion, in a circular orbit about the stationary journal.

^bZero load only momentary since half-frequency whirl occurred.

of the pumping action of the herringbone grooves.

As shown in table III, bearing MP-3 ran for 490 minutes and showed little wear (fig. 8). The slight scoring of the journal was probably caused by a small contaminant particle. Bearing MP-4 seized after 90 minutes because a line heater expansion pushed the test vessel and overloaded, or cocked, the bearing.

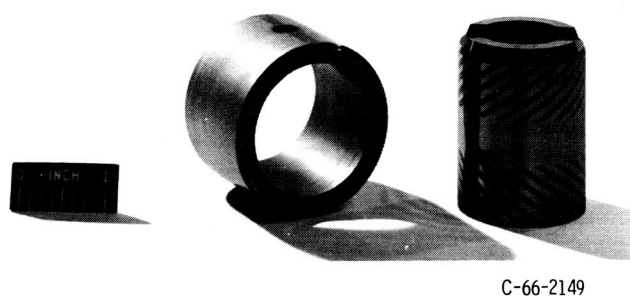


Figure 8. - Plain bearing MP-3 against herringbone-groove journal K-14 after test. C-66-2149

Tilting-Pad Bearings

Five tilting-pad bearings having a three-pad configuration were tested in sodium at 500° and 800° F at speeds from 3000 to 12 000 rpm and loads from zero to 31.1 pounds per square inch. These results are summarized in table IV. Of the five bearings tested, one seized because of overloading (bearing T-2), and one seized because of a combination of insufficient clearance and incompatible bearing and journal material (bearing T-1A). The wear on the unloaded pad of bearings T-1 and T-2A1 was probably caused by insufficient preload which resulted in pad flutter.

The various preload coefficients investigated are listed in table IV. Although the results were inconclusive because of the limited number of tests, it appeared that tilting-pad bearings with large radial clearances before preload (0.0028 and 0.0036 in.) and high preload coefficients (0.50 and 0.72) yielded the best results, as far as wear of pads is concerned. (These bearings had radial clearances at pivots of 0.0014 and 0.0010 in., respectively.)

Figure 9 shows a tilting-pad bearing that failed as the result of overloading.



Figure 9. - Failure due to overloading. Tilting-pad bearing T-2 against journal J-12.

TABLE IV. - RESULTS OF TESTS OF TILTING-PAD BEARINGS IN SODIUM

Bearing Number	Bearing Material	Journal		Bearing type	Test temperature, °F	Radial clearance at test temperature, in.		Preload coefficient	Journal speed-range tested, rpm	Unit load-range tested, psi	Total test time, min	Observed instability	Remarks
		Number	Material			At zero preload, C_{ro}	At pivot location after preload ^a , C_p						
T-1	Inconel	J-10	Stellite Star J	Three tilting pad	500	0.0021	0.0017	0.19	5 000 to 11 000	4.5 to 6.7	175	None present	Little wear observed, with most wear on unloaded pad. Pivot surfaces showed slight surface damage.
T-2	Inconel	J-12	Stellite Star J	Three tilting pad	500	0.0011	0.0007	0.36	5 000 to 9 000	4.5 to 31.1	311	None present	Bearing seized at 9000 rpm at 31.1 psi because of overload-ing. Loaded pad showed most wear.
T-2A1	Inconel	J-13	Stellite Star J	Three tilting pad	500	0.0028	0.0014	0.50	3 000 to 11 000	0 to 8.9	590	None present	Unloaded pad showed most wear indicating possible insufficient preload. Journal showed light wear. Pivots showed mating-surface damage.
T-3	Hastelloy X	J-14	Stellite Star J	Three tilting pad	500 and 800	0.0036	0.0010	0.72	2 000 to 12 000	0 to 17.8	1013	None present	Little wear on all shoes. Pivots showed mating-surface damage. Clearance at 800° F was not appreciably different from 500° F value.
T-1A	Inconel	HX-8	Hastelloy X	Three tilting pad	800	0.0010	0.0003	0.70	5 000 to 8 000	4.5	175	None present	Bearing seized when higher load than 4.5 psi was attempted, probably because of tight clearance and incompatible materials. Wear evenly distributed between pads.

^aMeasured by observation of oscilloscope pattern as the test vessel was moved by hand, to the limits of its outward motion, in a circular orbit about the stationary journal.

^bCalculated. Fig. 2.

Pads B and C were the loaded pads, with most of the wear shown on the leading edge of pad C. Analysis of the wear pattern on the outer edges of all three pads would indicate that the pads had rolled during operation (fig. 10). The surface damage to unloaded pad A was attributed to the failure of this bearing when wear debris was transferred completely around the bearing just prior to seizure.

Bearing torque data obtained from tilting-pad bearings at zero load and at 10-pound radial load are shown in figures 11(a) and (b), respectively. These data are shown compared with the theoretical laminar torque calculated from the Petroff equation

$$T_l = \frac{\mu \pi^2 D^3 L N}{120 C_r}$$

and the theoretical turbulent torque calculated from the equation given by Smith and Fuller in reference 5, where $T_t = T_l (0.039 \text{ Re}^{0.57})$ (All symbols are defined in the appendix.) The theoretical torques are for a full circular bearing with no eccentricity; therefore, they are only rough approximations for a tilting-pad bearing, and only for zero preload. Bearing torque values indicated that turbulent flow conditions prevailed over the greater part of the speed range tested, primarily because of the low sodium viscosity. The experimental transitional speed, where the bearing passes from the laminar to the turbulent regime, occurred at a higher speed than that predicted by theory (critical transitional speed N_T), perhaps because this transition occurs over a range of speeds rather

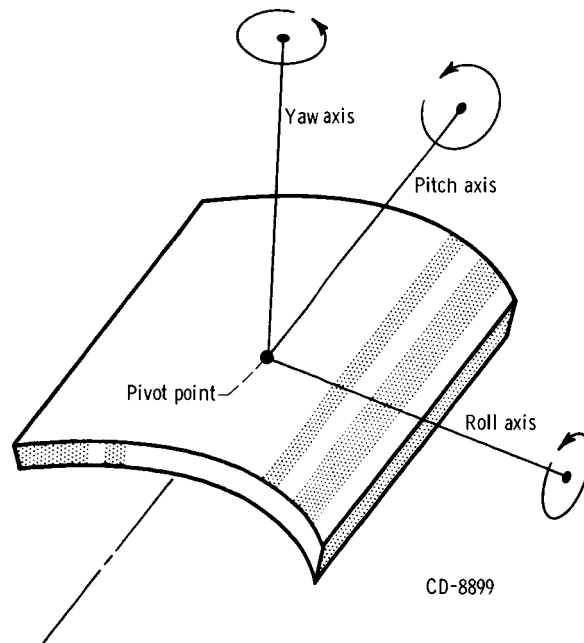


Figure 10. - Terminology used to define pad motions.

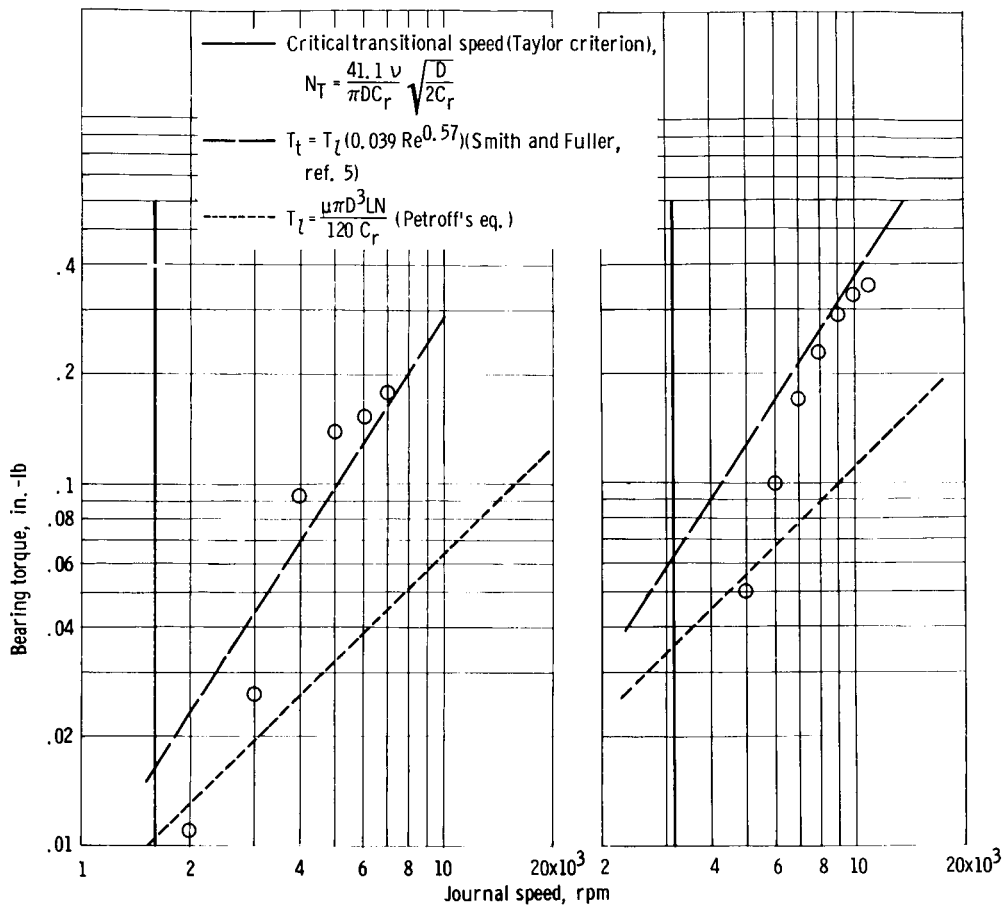


Figure 11. - Comparison of experimental and theoretical friction torques for three-pad tilting-pad bearing. Lubricant, 500° F sodium; journal material, Stellite Star J; nominal diameter, 1.5 inches; nominal length, 1.5 inches.

than at one definite speed. Similar results for the transition speed were reported in reference 6. No abrupt increase in torque readings was noticed when turbulent flow conditions were approached. The gradual increase in torque with speed made it difficult to specify exactly the speed at which full turbulence was attained.

Bearing Instability

The bearing instability of principal concern here is that known as one-half frequency whirl. Figure 12 illustrates simply the origin of the one-half frequency-whirl phenomenon in a full cylindrical bearing. When the shaft is displaced by a radial load from a concentric position with the bearing, a pressure buildup occurs in the fluid film. A force component F_w acting at right angles to the eccentricity e is produced and, if great

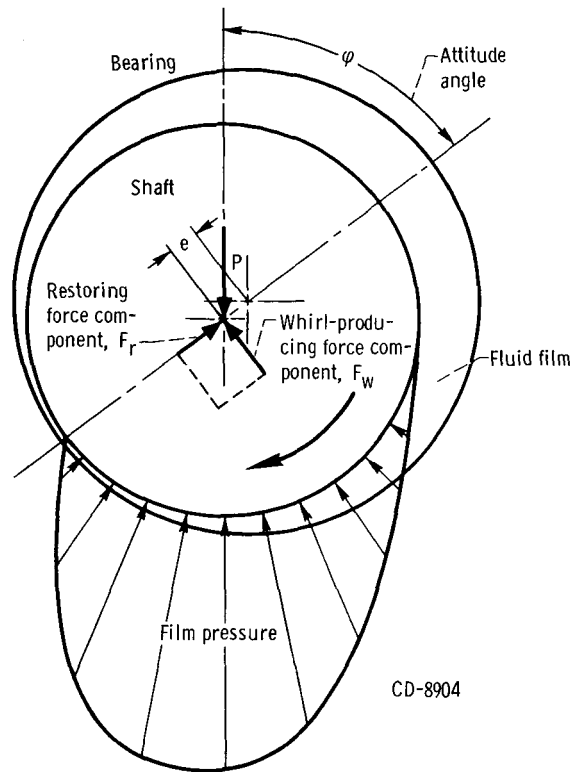


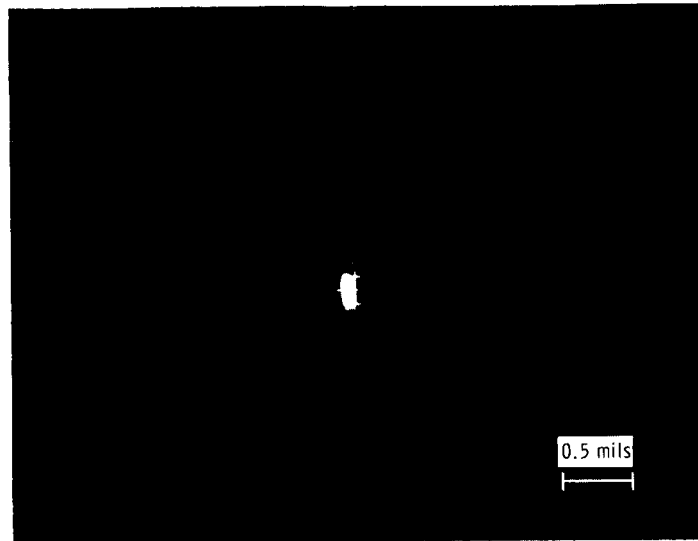
Figure 12. - Half-frequency-whirl phenomenon.

enough, will cause the shaft center to whirl about the bearing center at approximately one-half the speed of the shaft. Application of a heavier radial load to the bearing will decrease its attitude angle ϕ , and reduce the whirl-producing force component F_w to a value too small to sustain the one-half frequency whirl. Thus, application of a heavier radial load results in stable operation.

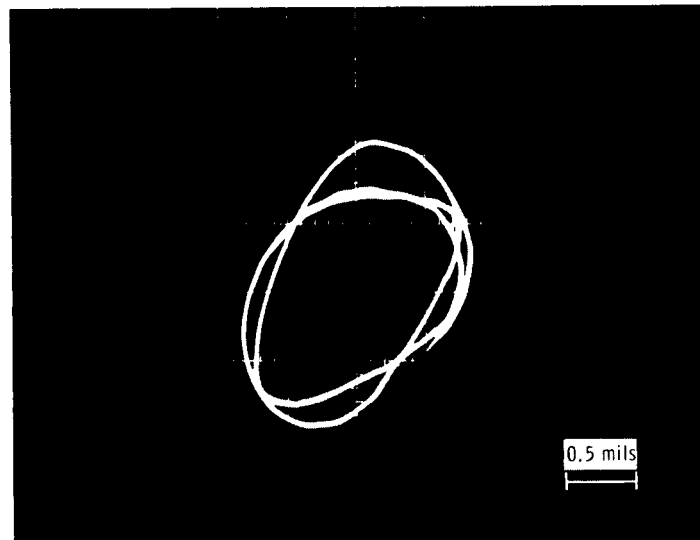
Figure 13 shows oscilloscope traces of bearing motion with a two-axial-groove bearing in sodium at 500° F with a 10-pound radial load. At 4100 rpm, the trace indicated stable bearing operation (fig. 13(a)). When the speed was increased to 5000 rpm, however, the increase in attitude angle was sufficient to sustain half-frequency whirl. The whirl pattern observed on the oscilloscope screen is shown in figure 13(b)). If the bearing were allowed to operate unstably, the supporting film between the bearing and journal would soon break down, and the bearing would eventually fail.

One of the most undesirable characteristics of the two- and three-groove bearings was instability. The result of such instability is clearly shown in figure 14. Test bearing J-2 is shown in this figure after 257 minutes of operation at a unit bearing load of 11 pounds per square inch in 500° F sodium under half-frequency-whirl conditions. The excessive wear shown is the result of unstable bearing operation.

Of the 14 two- and three-groove cylindrical bearings tested, 5 showed excessive



(a) Stable operation at 4100 rpm; 10-pound radial load.

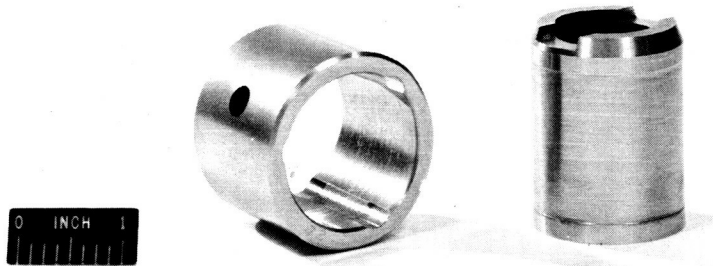


(b) Unstable operation (half-frequency whirl) at 5000 rpm; 10-pound radial load.

Figure 13. - Oscilloscope traces of bearing motion of two-axial-groove bearing in sodium at 500° F. Bearing M-1 against journal K-6. Diametral clearance, 0.0020 inch.

wear because of half-frequency whirl, and 1 seized because of this instability.

One of the three-groove bearings (M-9 in table II, pp. 10 and 11) was loaded sufficiently at each speed throughout its evaluation to keep it running stably. After 290 minutes of running time in 500° F sodium, the bearing was removed. No measurable wear was present on either the journal or the bearing. The maximum load on this bearing was 26.7 pounds per square inch at a maximum speed of 10 000 rpm, which indicates that a three-groove cylindrical bearing will run successfully in sodium if it is properly loaded to suppress half-frequency whirl.



C-65-1556

Figure 14. - Wear due to unstable bearing operation (one-half-frequency whirl). Stellite star J bearing J-2 against Hastelloy X journal HX-C.

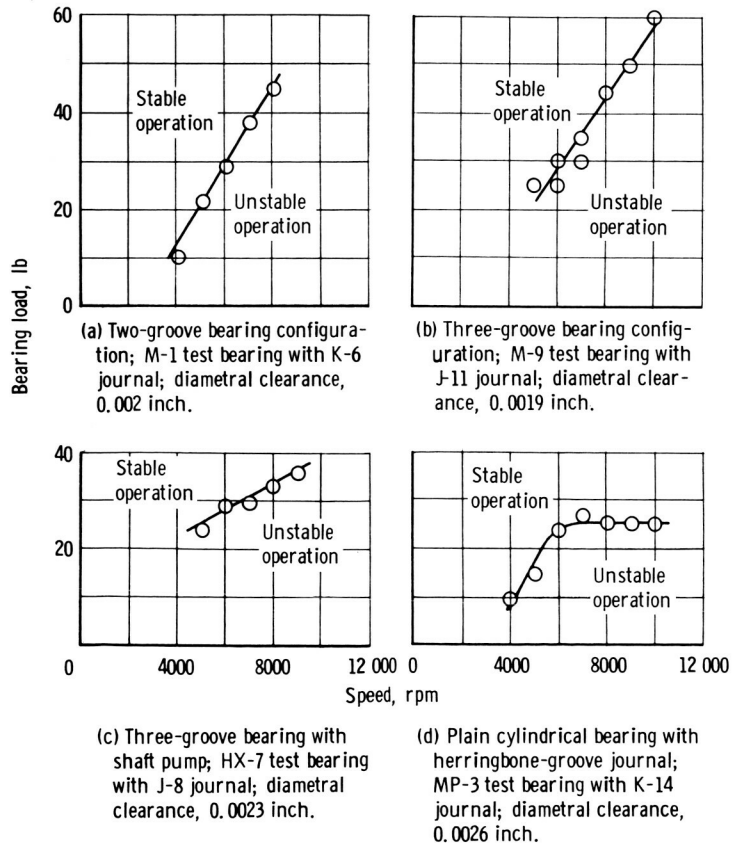


Figure 15. - Comparison of four different bearing and journal configurations at speed and load at which half-frequency whirl is initiated.

Theory indicates that herringbone-groove bearings operate at considerably lower attitude angles with more favorable stability characteristics than do smooth bearings. This type of bearing assembly was indeed more stable than the two- and three-axial-groove bearings and plain journal assemblies. However, the herringbone-groove bearing assembly did show evidence of half-frequency whirl at low load conditions. A more judicious design of the herringbone-groove journal might lead to a bearing that would be stable even at zero-load conditions. Such a bearing has been run at zero load in air to 60 000 rpm without any evidence of half-frequency whirl (ref. 7).

Figure 15 shows the stability characteristics of four different bearing configurations. The data for these curves were obtained by running the bearings at various speeds and gradually decreasing the load until indications of half-frequency whirl were observed. This load plotted against its corresponding speed resulted in the stability curves shown. At any condition above the curve, stable operation resulted; below the curve, half-frequency whirl resulted. For all bearing types, higher operating speeds require higher loads to maintain stable operation.

Figure 16 shows the relative stability of the four different cylindrical bearing configurations tested. The two- and three-axial-groove bearing configurations were the least stable of the four because they required the highest load at any specific speed to maintain stable operation. The plain bearing with a herringbone-groove journal was the most stable of the four because it required the lowest load at a given speed to maintain stability. Axial-grooved bearings appeared to require a linear increase in load with speed for stable operation, whereas the herringbone-groove bearing was stable at a unit load of 11.1 pounds per square inch at speeds from 7000 to 10 000 rpm.

Experimental data on the threshold of instability of two- and three-axial-groove bearings correlated well with the theoretical curves reported in reference 8.

Figure 17 shows theoretical curves of dimensionless critical rotor mass plotted against the Sommerfeld number for a 100° partial-arc bearing and a plain cylindrical (full circular) journal bearing for Reynolds numbers from 0 to 1663. The data points for the two-axial-groove and three-axial-groove bearings generally fall between the curves, which indicates good correlation.

The procedure for determining the threshold speed is to calculate the dimensionless rotor mass M_{cr} . Entering the value thus calculated in figure 17 and determining the corresponding Sommerfeld number yields the threshold speed, that is, the rotor speed at onset of instability.

The tilting-pad bearings were the most stable of the five configurations tested. Tilting-pad bearings T-3 and T-2A1 were run to 12 000 rpm and 11 000 rpm, respectively, at zero load without exhibiting any half-frequency-whirl instability. Although not tested at zero load, the remaining three bearings of the tilting-pad

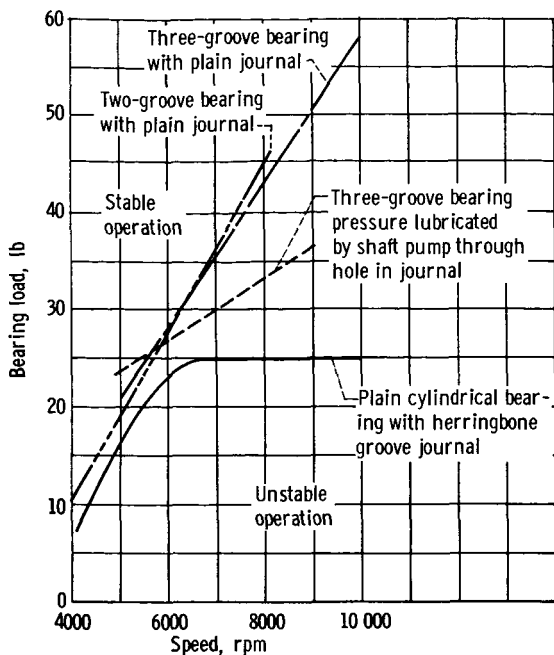


Figure 16. - Comparison of four different bearing and journal configurations at speed and load at which bearing instability is initiated.

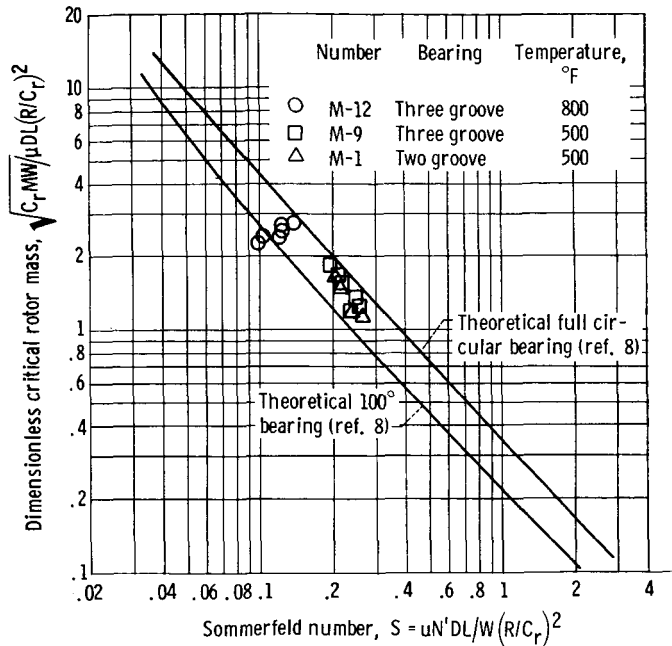


Figure 17. - Dimensionless critical rotor mass as function of Sommerfeld number at onset of half-frequency-whirl instability for plain cylindrical and 100° partial-arc bearings operating with turbulent film. Ratio of bearing length to diameter, 1; Reynolds number, 0 to 1663.

group showed good stability at light loads of 4.5 pounds per square inch to speeds of 11 000 rpm.

Material Compatibility

The bearing and journal material combinations that had good wear and seizure properties in sodium to 800° F are shown in figure 18. Stellite Star J material mated with Hastelloy X, titanium carbide (K184B), or Inconel had the best wear and seizure resistance. Also titanium carbide (K184B) mated with molybdenum - 0.5 percent titanium showed excellent promise. Materials such as Hastelloy X and Inconel, which have a high nickel content, were prone to catastrophic seizure when paired in a bearing and journal combination.

In figure 19(a), the results of a seizure of a three-axial-groove bearing due to an incompatible bearing and journal material combination are shown. The bearing material was molybdenum - 0.5 percent titanium, and the journal material was Hastelloy X. The surface of the journal shows galling, which is typical of this type of failure.

Another example of the results of pairing incompatible materials is shown in figure 19(b). The bearing material was Inconel and the journal material was Hastelloy X, both high in nickel content. Seizure resulted in galling of the pads and journal. The

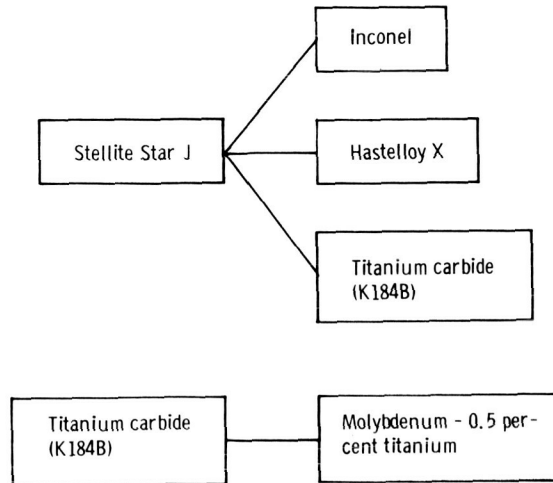
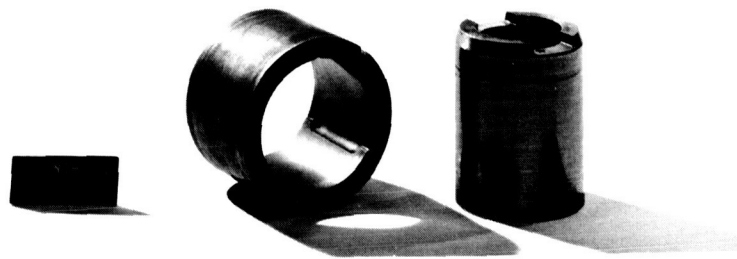
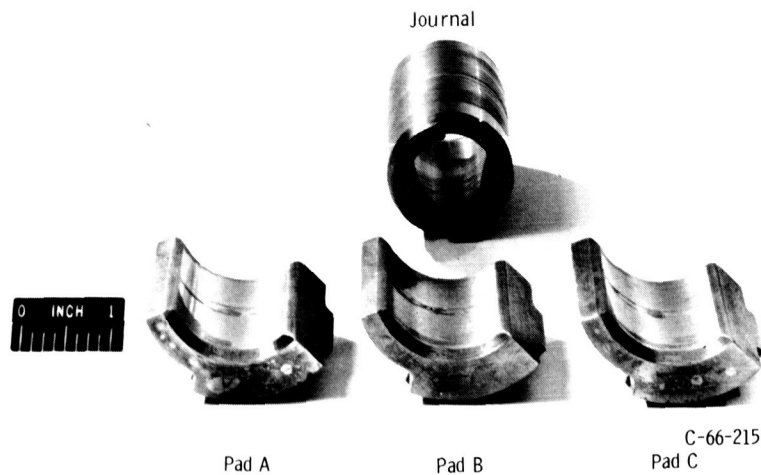


Figure 18. - Bearing and journal material combinations that have good resistance to wear and seizure in sodium to 800° F.



C-66-2148

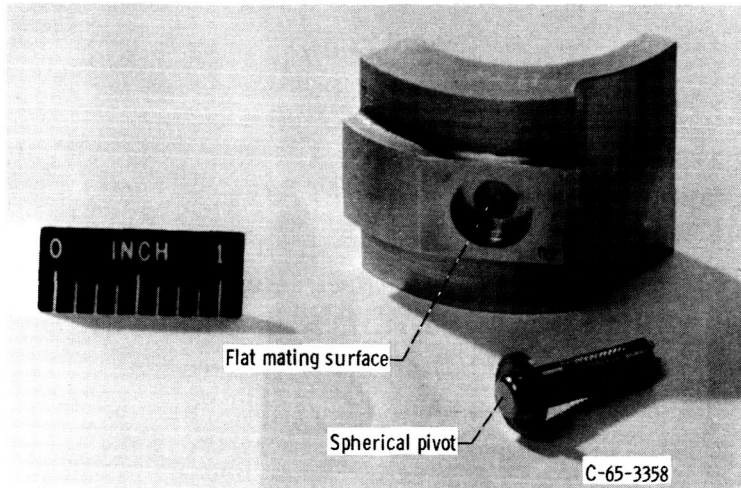
(a) Three-axial-groove molybdenum -0.5 percent titanium bearing M-11 against Hastelloy X journal HX-7.



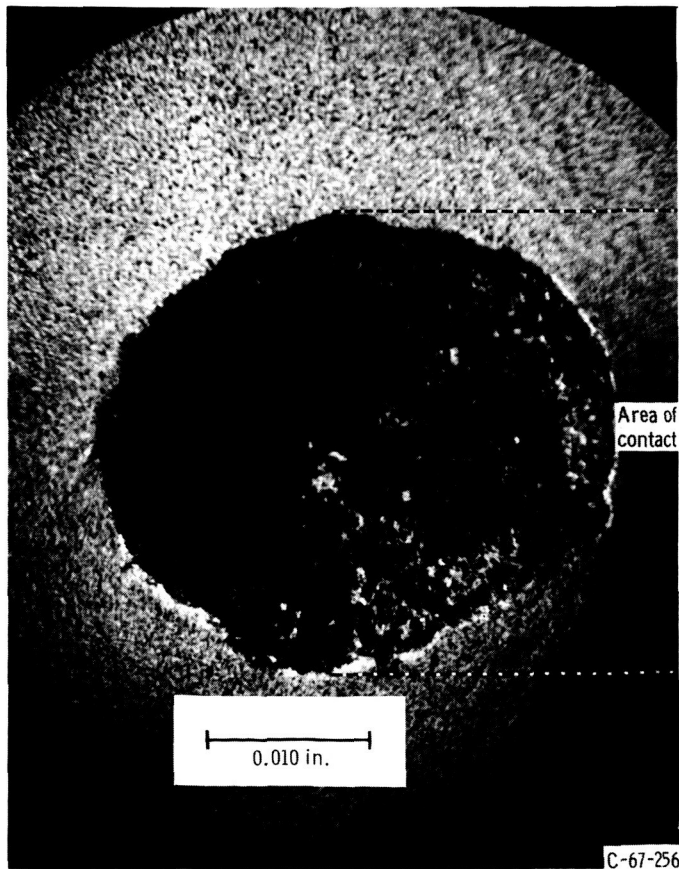
C-66-2151

(b) Tilting-pad-Inconel bearing T-1A against Hastelloy X journal HX-8.

Figure 19. - Seizure due to incompatible material combination.



(a) Spherical pivot and flat mating surface in pad.



(b) Surface damage to spherical pivot.

Figure 20. - Tilting-pad-bearing pivot after operation in sodium. Both spherical pivot and flat mating surface of titanium carbide (K162B).

bearing radial clearance at the pivots of 0.0003 inch would not allow larger particles to pass through the bearing without initiating surface damage. With a poor combination of materials, galling, severe surface damage, and possible seizure quickly follow the initial surface damage.

Figure 14 (p. 21) shows an example of mating materials with good compatibility. The combination of Stellite Star J and Hastelloy X material showed excellent seizure resistance. This bearing and journal combination did not seize even after the excessive wear shown in the figure, although the bearing was deliberately operated under half-frequency-whirl conditions for approximately 90 minutes.

Figure 20(a) shows the pivot arrangement used on the tilting-pad bearings, a spherical pivot against a flat mating surface (shown schematically in fig. 5, p. 9). A typical example of surface damage to the pivot that was observed in some tests, even short runs at light load, is shown in figure 20(b). This damage occurred with both the titanium carbide (K162B) and the Stellite Star J pivot materials, which were always mated against themselves. As shown in table IV (p. 16), bearing T-1 ran for 175 minutes with a maximum load of 15 pounds on the pivot.

This resulted in a Hertz stress of only 52 600 pounds per square inch which, however, was sufficient to cause slight damage to the pivot surface.

SUMMARY OF RESULTS

A series of hydrodynamic journal-bearing experiments was run in sodium at 500^o and 800^o F at speeds to 12 000 rpm and loads to 31.1 pounds per square inch. Five different configurations were tested: cylindrical bearings with two and three axial grooves, a three-axial-groove bearing pressure fed from a hole in the journal, plain cylindrical bearings with herringbone-groove journals, and tilting-pad bearings with three pads. The bearing bore in all cases was 1.5 inches and all bearings had a length to diameter ratio of 1. The following results were obtained:

1. The tilting-pad bearings were the most stable, followed in order by a plain cylindrical bearing with a herringbone-groove journal, a three-axial-groove bearing pressure fed from an axial shaft pump through a hole in the journal, and three- and two-axial groove bearings.

2. Stellite Star J material mated with Hastelloy X, titanium carbide (K184B), or Inconel had the best resistance to wear and seizure. Also titanium carbide (K184B) mated with molybdenum - 0.5 percent titanium showed excellent promise. Materials with a high nickel content, such as Hastelloy X and Inconel, were prone to catastrophic seizure when paired in a bearing and journal combination.

3. Data on the threshold of instability of cylindrical, grooved bearings obtained from this investigation compared favorably with predicted theoretical values.

4. Actual bearing torque values (for the tilting-pad bearings) agreed favorably with turbulent flow theory, indicating that turbulent flow conditions prevailed over the greater portion of the speed range tested, primarily because of the low sodium viscosity. Critical transitional speed from laminar to turbulent flow occurred at a higher speed than the theoretical Taylor criterion predicts.

5. No abrupt increase in torque readings was noticed when turbulent flow conditions were approached, indicating that the transition from laminar to turbulent flow occurs gradually over a range of Reynolds number rather than suddenly. The gradual buildup of torque made it difficult to specify exactly at which speed turbulence was initiated.

6. Surface damage of the tilting-pad bearing pivots was observed in some tests even after short runs at light pivot loads. The pivot configuration used in this investigation was a spherical pivot against a flat mating surface and the materials were titanium carbide (K162B) against itself and Stellite Star J against itself.

7. Although the results were inconclusive because of the limited number of tests, the tilting-pad bearings with large radial clearances before preload (0.0028 and

0.0036 in.) and high preload coefficients (0.50 and 0.72) appeared to yield the most favorable test results. (These bearings after preloading had radial clearances at the pivots of 0.0014 and 0.0010 in., respectively). The tilting-pad bearings were the most stable of the five configurations tested.

Lewis Research Center,
National Aeronautics and Space Administration,
Cleveland, Ohio, December 23, 1966,
120-27-04-03-22.

APPENDIX - SYMBOLS

a	preload	P	radial load, lb
C_p	bearing radial clearance at pivot location after preload, $R_p - a - R_s$	R	bearing radius, in.
C_r	bearing radial clearance, in.	Re	Reynolds number, $\pi DN\rho C_r/60\mu$, dimensionless
C_{ro}	bearing radial clearance at zero preload, $R_p - R_s$	R_p	radius of pad, in.
D	bearing diameter, in.	R_s	radius of shaft, in.
e	eccentricity	S	Sommerfeld number, $(\mu N'DL/W)(R/C_r)^2$
F_r	restoring force component	T_ℓ	Petroff's torque for laminar flow and zero load, $\mu\pi^2 D^3 LN/120C_r$
F_w	whirl-producing force component	T_t	turbulent torque (Smith and Fuller, ref. 5), $T_\ell(0.039 Re^{0.57})$
g	acceleration due to gravity, in./sec ²	W	bearing load, lb
L	bearing length, in.	W_r	load due to rotor mass, Mg, lb
M	rotor mass per bearing, W_r/g , (lb)(sec ²)/in.	β	groove angle measured from perpendicular to journal axis, deg
M_{cr}	dimensionless critical rotor mass, $\sqrt{C_r MW/\mu DL}(R/C_r)^2$	μ	absolute lubricant viscosity, reyns, (lb)(sec)/in. ²
N	journal speed, rpm	ν	kinematic viscosity, (cS)(in. ²)/sec
N'	journal speed, rps	ρ	lubricant mass density, (lb)(sec ²)/in. ⁴
N_T	critical transitional journal speed from laminar to turbulent regime, $(41.1 \nu)/\pi DC_r \sqrt{D/2C_r}$, rps	φ	attitude angle

REFERENCES

1. Slone, Henry O. ; and Lieblein, Seymour: Electric Power Generation Systems for Use in Space. Advances in Aeronautical Sciences. Vo. 4. Th. von Kármán and H. L. Dryden, eds., Pergamon Press, 1962, pp. 1131-1152.
2. Basham, Samuel J. ; Stang, John H. ; and Simons, Eugene M. : Corrosion Screening of Component Materials for NaK Heat Exchange Systems. Paper presented at the Nuclear Engineering and Science Conference, Chicago, AIChE, Mar. 17-21, 1958.
3. Apkarian, Harry: Investigation of Liquid Metal Lubricated Bearings. Rep. No. 50GL231, General Electric Co., Nov. 27, 1950.
4. Cook, W. H. : Corrosion Resistance of Various Ceramics and Cermets to Liquid Metals. Rep. No. ORNL-2391, Oak Ridge National Lab., June 15, 1960.
5. Smith, M. I. ; and Fuller, D. D. : Journal-Bearing Operation at Super-laminar Speeds. ASME Trans., vol. 78, no. 3, Apr. 1956, pp. 469-474.
6. Stahlhuth, Paul H. ; and Trippett, Richard J. : Liquid Metal Bearing Performance in Laminar and Turbulent Regimes. ASLE Trans., vol. 5, no. 2, Nov. 1962, pp. 427-436.
7. Malanoski, S. B. : Experiments on An Ultra-Stable Gas Journal Bearing, Paper No. 66-LUB-6, ASME, 1966.
8. Lund, J. W., ed. : Design Handbook for Fluid Film Type Bearings. Part III of Rotor-Bearing Dynamics Design Technology. Rept. No. MTI-65TR14 (AFAPL-TR-65-45, pt. III, DDC No. AD-466392), Mechanical Technology, Inc., May 1965.

"The aeronautical and space activities of the United States shall be conducted so as to contribute . . . to the expansion of human knowledge of phenomena in the atmosphere and space. The Administration shall provide for the widest practicable and appropriate dissemination of information concerning its activities and the results thereof."

—NATIONAL AERONAUTICS AND SPACE ACT OF 1958

NASA SCIENTIFIC AND TECHNICAL PUBLICATIONS

TECHNICAL REPORTS: Scientific and technical information considered important, complete, and a lasting contribution to existing knowledge.

TECHNICAL NOTES: Information less broad in scope but nevertheless of importance as a contribution to existing knowledge.

TECHNICAL MEMORANDUMS: Information receiving limited distribution because of preliminary data, security classification, or other reasons.

CONTRACTOR REPORTS: Scientific and technical information generated under a NASA contract or grant and considered an important contribution to existing knowledge.

TECHNICAL TRANSLATIONS: Information published in a foreign language considered to merit NASA distribution in English.

SPECIAL PUBLICATIONS: Information derived from or of value to NASA activities. Publications include conference proceedings, monographs, data compilations, handbooks, sourcebooks, and special bibliographies.

TECHNOLOGY UTILIZATION PUBLICATIONS: Information on technology used by NASA that may be of particular interest in commercial and other non-aerospace applications. Publications include Tech Briefs, Technology Utilization Reports and Notes, and Technology Surveys.

Details on the availability of these publications may be obtained from:

SCIENTIFIC AND TECHNICAL INFORMATION DIVISION
NATIONAL AERONAUTICS AND SPACE ADMINISTRATION
Washington, D.C. 20546